Streamline Extrapolation Technique for Subsonic Outflow Boundary Conditions in DSMC Simulations

Özhan H. Turgut and M. Cevdet Çelenligil

Department of Aerospace Engineering, Middle East Technical University, 06531 Ankara, Türkiye

Abstract. A subsonic outflow boundary condition technique is developed for the DSMC calculations. In this scheme, the macroscopic boundary properties are extrapolated from the interior domain along the streamline trajectories using the Neumann boundary conditions. Simulations are performed for the two-dimensional subsonic rarefied flows over an infinitely thin plate (either finite or semi-infinite) with zero angle of attack at constant pressure. Flows with a Mach number of 0.102 and 0.4 and a Reynolds number varying between 0.063 and 246 are investigated, covering most of the transitional regime between the free-molecule and the continuum limits. The computed results are in very good agreement with the available experimental data and theoretical results.

INTRODUCTION

Micro-electromechanical systems (MEMS) are becoming more commonplace in today's technology advancements, but a number of features concerning these systems are not well understood, such as the gas motion in these systems. These subsonic flows are rarefied because the mean free path of the gas molecules is comparable to the dimensions of these micron-size devices even under atmospheric conditions.

Subsonic rarefied flows have been studied in the past using the direct simulation Monte Carlo (DSMC) method of G. A. Bird [1] by several researchers for channel flows [2,3]. On the other hand, very few simulations have been reported in the literature on the subsonic rarefied flat-plate flows [4] as a result of some additional difficulties involved in the simulation of these flows. In flat-plate flows, the top part of the domain is an open boundary and, hence, simulations usually require much larger computational domains as compared to channel flows. Naturally, the solutions for flat plates are also more sensitive to the stipulated open boundary conditions. This is complicated by the fact that the simple freestream and vacuum boundary conditions conventionally used at the open boundaries of the hypersonic flows [5] are not applicable in subsonic flows, and one has to resort to extrapolations from the interior domain to determine some of the boundary properties. The scarcity of experimental data for these subsonic rarefied flows is an obstacle for the verification of the extrapolated boundary conditions. Isolating the statistical scatter from the mean quantities is another difficulty in low speed rarefied flows, as this requires large samples.

In the present research, subsonic rarefied flows over a flat plate are investigated. The two-dimensional G2 DSMC code of G. A. Bird is used in the simulations, and the inflow/outflow boundary conditions of the code are modified.

BOUNDARY CONDITIONS

For the subsonic DSMC simulations, several alternatives may be considered for the open boundary conditions. One option may be to use the freestream conditions directly, but this is suitable only if the domain is very large. Another choice is to use Dirichlet boundary conditions if the flow properties at the open boundaries are known in advance, but this is usually not possible. Consequently, for these flows, some of the boundary properties need to be extrapolated from the interior domain. A commonly used technique is to apply "far-field" conditions with characteristics if isentropic assumption holds between the open boundaries and the freestream.

In the present simulations, characteristics are used at the subsonic inflow boundaries since the isentropic assumption is viable. According to one-dimensional inviscid characteristic formulation, at the subsonic inflow boundaries, two characteristics come from the freestream and one characteristic comes from the interior domain.

Hence, in this study, one property (one of the Riemann invariants) is taken from the interior domain and the rest of the properties (with the other Riemann invariants) are taken from the freestream to determine the inflow properties. On the other hand, for the subsonic outflow boundaries, an extrapolation technique is developed because the use of characteristics is not always suitable as in the case of semi-infinite plate flows or simulations on small domains. In the present calculations, one property (pressure) is taken from the exterior, and the rest of the properties are extrapolated from the interior domain. Extrapolations are done along the streamline trajectories together with the Neumann boundary conditions, $\partial\varphi/\partial\xi = 0$, where φ denotes macroscopic quantities and ξ is in the streamline direction. Several other boundary conditions are also tested [6], but the most satisfactory results are obtained with the present extrapolation technique.

In this technique, a "ghost cell" is introduced adjacent to each open boundary cell and extrapolations are made along the streamline trajectory passing through the center of the ghost cell. In the calculations, a rectangular domain is used and the top and right edges of this domain are outflow boundaries. Consider the right boundary as shown in Fig. 1. Assuming that the streamlines are linear at the boundaries, one can draw the streamlines passing through the cell centers A and B with the help of velocity vectors. For this method to work, the center of the ghost cell should lie in between these two streamlines. If this condition is not met, a searching process is started considering other boundary cells until it is satisfied. Supposing that the center of the ghost cell O lies in between the streamlines passing through points A and B, the macroscopic properties at O are calculated by an interpolation based on the shortest distances between point O and these streamlines (*i.e.* S_A and S_B). Using a weighting factor, $\alpha = S_A/(S_A+S_B)$, the macroscopic quantities, φ, of the ghost cell O are calculated from $\varphi_O = (1-\alpha)\,\varphi_A + \alpha\,\varphi_B$.

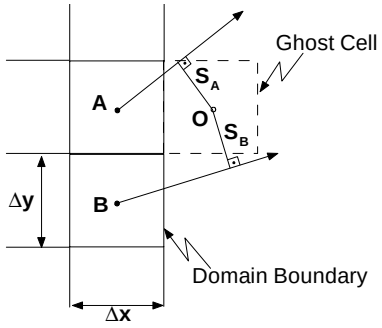

FIGURE 1. Streamline extrapolation.
(Arrows represent velocity vectors.)

RESULTS AND DISCUSSION

Two-dimensional subsonic rarefied flows over an infinitely thin flat plate with zero angle of attack at constant pressure are investigated. In the computations, a rectangular domain is used and both finite and semi-infinite plate configurations are examined as illustrated in Fig. 2. The plate is located at y = 0 with its leading edge at x = 0, and the length of the plate in the computational domain is denoted by L. The plate temperature is set to 299.4 K.

In the freestream, two-species air (O_2 and N_2) is used with mole fractions of 21.2% and 78.8%, respectively. The freestream conditions considered in this study are listed Table 1 where U_∞, n_∞, M, Kn and Re are the velocity component in the x-direction, number density, Mach number, Knudsen number and Reynolds number, respectively. Also, the velocity component in the y-direction, V_∞, is zero and the temperature is 299.4 K.

In the simulations, a variable-hard-sphere model [7] is applied to the molecular collisions with a temperature-viscosity exponent of 0.74, a reference temperature of 298.15 K, and a reference diameter of 4.02×10^{-10} m. Larsen-Borgnakke model is employed to control the energy exchange between translational and other modes. The rotational and vibrational relaxation collision numbers are 5 and 50, respectively. Full thermal accommodation and diffuse reflection are assumed for the gas-surface interactions. Nearly 10 representative molecules are used in each cell. For the Kn = 0.02 calculations, cell sizes in the x- and y-directions (*i.e.* Δx and Δy, respectively) are approximately equal to the local mean free path. In the more rarefied cases, Δx and Δy are smaller than the local mean free path.

(a) Finite plate (b) Semi-infinite plate

FIGURE 2. Schematic of the domains.

TABLE 1. Freestream conditions.

U_∞ [m/s]	n_∞ [molecule/m^3]	M	Kn*	Re*
35.26	2.36×10^{25}	0.102	0.02	6.26
35.26	2.36×10^{24}	0.102	0.2	0.626
35.26	2.36×10^{23}	0.102	2	0.0626
138.74	2.36×10^{26}	0.4	0.002	246.27
138.74	2.36×10^{25}	0.4	0.02	24.627
138.74	2.36×10^{24}	0.4	0.2	2.4627
138.74	2.36×10^{23}	0.4	2	0.24627

* based on a length scale of 2.792×10^{-6} m.

On the other hand, for the densest test case, *i.e.* Kn = 0.002, although Δy is equal to the local mean free path, Δx is taken as five times that to reduce the excessive computational time. Then, to get a feel for the error caused by these large cells, the Kn = 0.02 calculations are repeated with Δx five times the local mean free path, and it is observed that the results change only a little (*e.g.* the drag coefficient changes by 3%).

Various flow simulations with finite and semi-infinite plate configurations are performed and results are presented in Figs. 3-14. (In these figures, the plate is located between x/L = 0 and 1. Also, sample sizes for the simulations are not the same and, hence, statistical scatter may vary on the results.) Figures 3-6 present results for a finite plate with $L = 2.792\times10^{-6}$ m at M = 0.4 for the freestream conditions listed in rows 4-7 of Table 1 (which are obtained by varying the freestream number density and keeping all other properties the same). The "collisionless" flow results in the figures are achieved by eliminating the intermolecular collisions in the Kn = 2 simulations. The size of the domain is varied with the degree of rarefaction. For the Kn = 0.02 case, the domain's upstream and downstream lengths and its height are 4L which are increased to 8L for the more rarefied cases. For the Kn = 0.002 calculations, domain's upstream and downstream lengths are L and its height is L/2. Figures 5 and 6 show the pressure and skin friction coefficients, $C_p = (p-p_\infty)/(0.5\rho_\infty U_\infty^2)$ and $C_f = \tau/(0.5\rho_\infty U_\infty^2)$, respectively, where p_∞ is the freestream pressure, ρ_∞ is the freestream density and τ is the surface shear stress. The theoretical free-molecular values for C_p and C_f are 0 and 1.69, respectively, and the computed "collisionless" values (averaged over the surface) are very close to them (C_p is 0.00023 and C_f is within 1% error). Note that, $C_p = 0.1$ means that the surface pressure is roughly 1% different from the freestream value. The present calculations show that, as the flow density increases, the use of small domains can easily perturb the surface pressures by a few percent causing large variations on C_p, while C_f remains relatively unaffected. This is suspected in the present Kn = 0.002 results, and they are not included in Fig. 5. The effects of rarefaction are evident in the results, *i.e.* as the flow becomes more rarefied, the slip velocities increase, the boundary layer height and the disturbance field around the body is enlarged, and the pressure and skin friction coefficients approach the limiting free-molecular values. Note that in Fig. 3 although the slip velocities decrease from x = 0 to x = L/2 (as expected), they increase from x = L/2 to x = L due to the presence of the flow in the downstream region. The drag coefficients, $C_D = D/(0.5\rho_\infty U_\infty^2 L)$, of finite plate flow calculations are presented in Fig. 7 for all freestream conditions listed in Table 1. (D denotes the drag force.) Clearly, the results are in excellent agreement with the experimental data [8]. Note that the results in this figure change slightly with the Mach numbers, but as the rarefaction increases they converge to the same theoretical free-molecular value.

In Figs. 8-11, results are presented for flows about a semi-infinite plate. These are essentially repetitions of the finite plate calculations with the exception that the downstream regions are removed. Comparison of the results in these figures with those in Figs. 3-6 for the finite plate flows shows the effects of different downstream configurations on the simulations. In the present flows, density is nearly constant in the domain and comparison may be also made with the incompressible Blasius solution. However, it should be kept in mind that, in the Blasius solution uniform freestream velocity is assumed at the leading edge; whereas the present results indicate that when the upstream portion of the domain is taken into account, a velocity profile forms there. Also, experiments [8] show that the Blasius solution underpredicts the drag coefficients under rarefied conditions. Still, due to the lack of extensive experimental data, making comparison with it may be useful. In these figures, the Blasius solution is obtained using the freestream data of the Kn = 0.02 flow at M = 0.4. Notice that, according to the Blasius solution, pressure is constant and, hence, C_p on the surface is zero; whereas the present results in Fig. 10 are nonzero. However, it should be considered that, for the "collisionless" flow, a variation of 0.8 in C_p along the surface corresponds to approximately 8% deviation of the surface pressure from p_∞, and also, as the Knudsen number gets smaller (approaching the continuum) this deviation decreases.

In general, when extrapolation boundary conditions are used, some errors near the borders are accepted as long as the main flow in the rest of the domain is not distorted. In order to check this for the present technique, the semi-infinite plate calculations (for M = 0.102 and M = 0.4) with $n_\infty = 2.36\times10^{25}$ molecule/m^3 are repeated by doubling L and it is observed that the solutions are not distorted (as can be seen from Fig. 12).

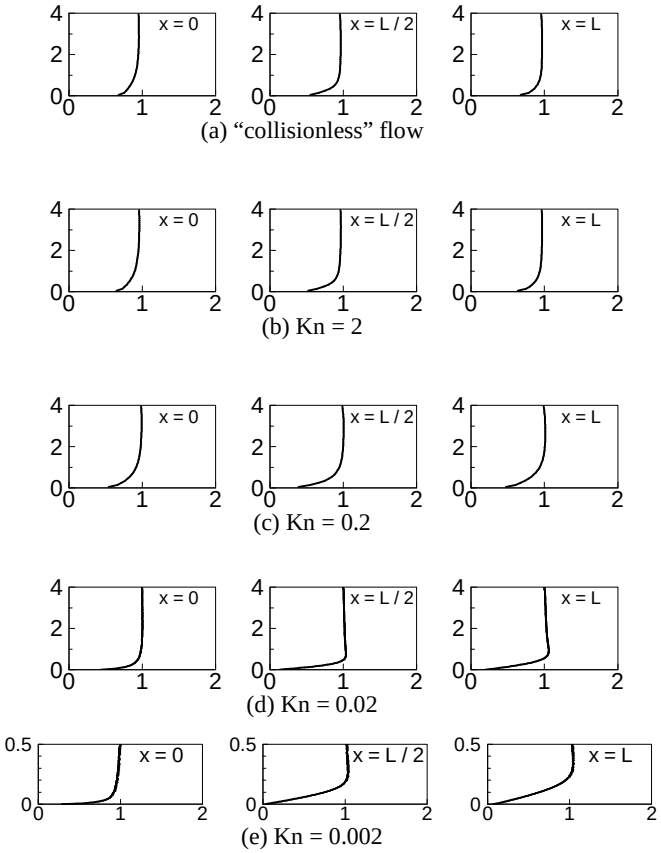

FIGURE 3. U profiles for finite plate (M = 0.4) (horizontal axes: U/U_∞, vertical axes: y/L).

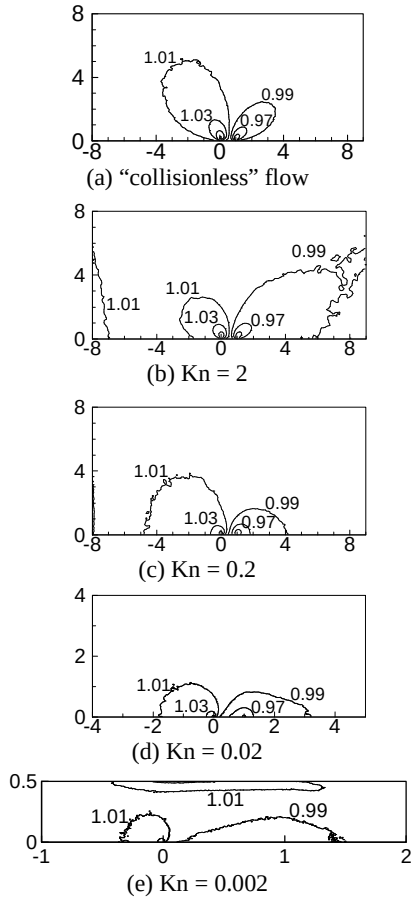

FIGURE 4. n/n_∞ contours for finite plate (M = 0.4) (horizontal axes: x/L, vertical axes: y/L).

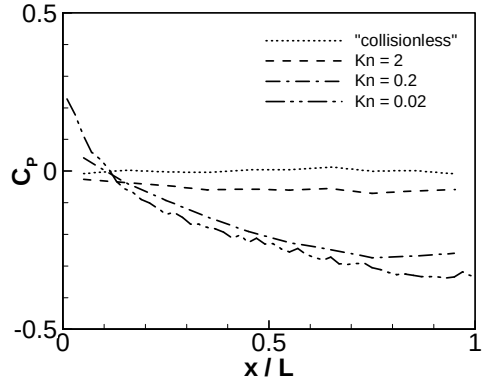

FIGURE 5. C_p distributions for finite plate (M = 0.4).

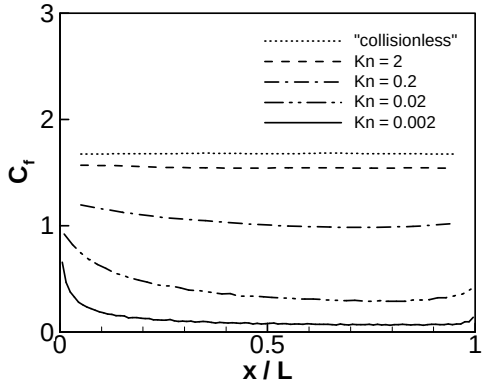

FIGURE 6. C_f distributions for finite plate (M = 0.4).

Also, comparison is made between the results of the present "collisionless" flow calculations and the theoretical free-molecule flow which provides an excellent opportunity for the verification of the present boundary conditions. Note that there is difference between the theoretical free-molecule flow and the present "collisionless" flow calculations. In the "collisionless" flow case, the present extrapolation boundary conditions are used; whereas in the theoretical free-molecule flow simulations, freestream conditions are stipulated to determine properties of the incoming molecules. The results of the two approaches for finite plate flow at M = 0.4 are in quite good agreement as can be seen from Figs. 13 and 4(a). Also, the "collisionless" $C_D \cdot M$ results for M = 0.102 and M = 0.4 calculations are within 1% error of the theoretical free-molecule flow value of 1.35 . This helps to build confidence on the present boundary conditions because all the boundary properties (except for the pressure) are determined by them.

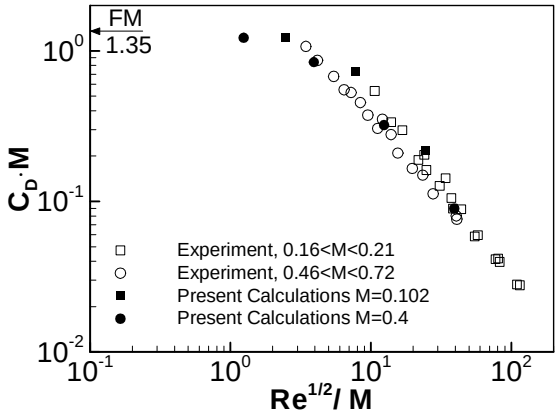

FIGURE 7. C_D for finite plate (FM : free-molecule).

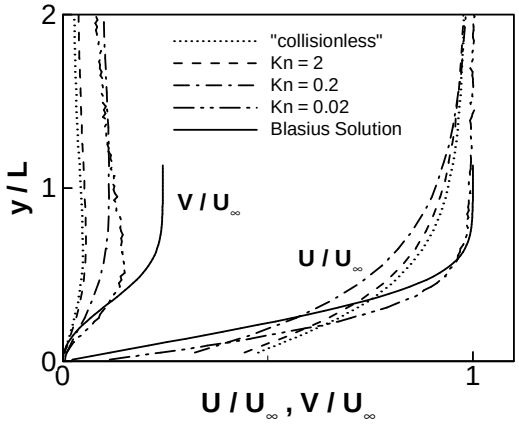

FIGURE 8. U, V at x = L/2 for semi-infinite plate (M = 0.4).

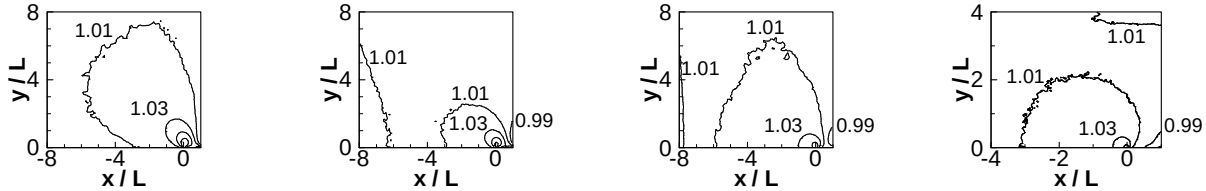

(a) "collisionless" flow (b) Kn = 2 (c) Kn = 0.2 (d) Kn = 0.02

FIGURE 9. n/n_∞ contours for semi-infinite plate (M = 0.4).

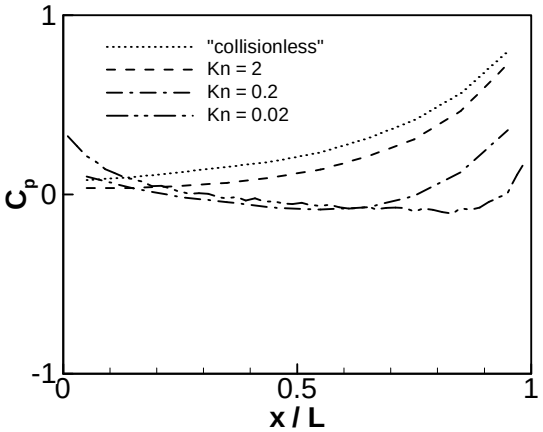

FIGURE 10. C_p distributions for semi-infinite plate (M = 0.4).

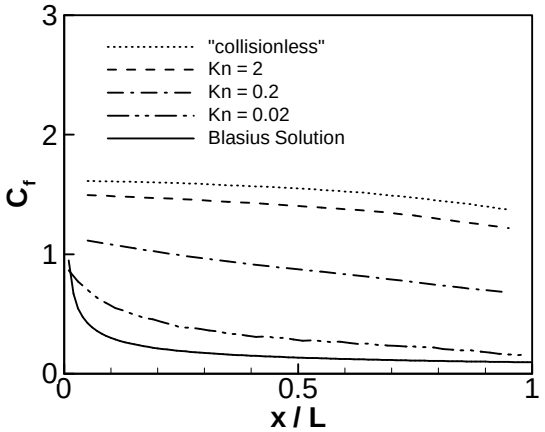

FIGURE 11. C_f distributions for semi-infinite plate (M = 0.4).

It should be also pointed out that, at the top boundary, the V velocity components are much smaller than U and, hence, the streamlines leave the domain with very small angles with respect to top boundary. Consequently, in using streamline extrapolation at the top boundary it may be necessary to extrapolate properties from the cells quite far away from the ghost cells. Besides, the streamlines at the top boundary sometimes direct into the domain during the computations, and the local outflow boundary condition is replaced by inflow boundary condition. (Clearly, these difficulties can be avoided by choosing the top boundary quite different from the outgoing streamlines.) It is noteworthy that the present boundary conditions perform remarkably well under these severe conditions, and produce satisfactory results.

The present boundary conditions are also successfully tested on several small computational domains. For example, Fig. 14 shows the results of the M = 0.4 "collisionless" finite plate flow calculations conducted on a small domain in which the upstream and downstream lengths and the height are L. Result of this flow are already presented in Fig. 4(a) using a computational domain which has an area approximately 45 times larger than the one used in Fig. 14. It can be seen that the results in Fig. 14 are still in quite good agreement with the ones in Fig. 4(a). The C_D results for the two calculations are only 1.5% different.

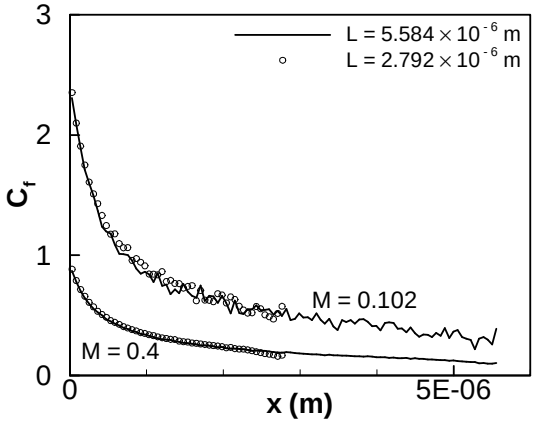

FIGURE 12. C_f distributions for various semi-infinite plate configurations ($n_\infty = 2.36\times10^{25}$ molecule/m^3).

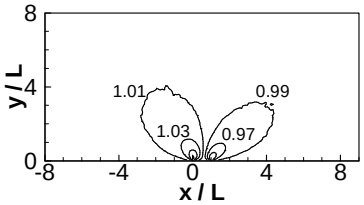

FIGURE 13. n/n_∞ contours for theoretical free-molecule flow (finite plate, M = 0.4).

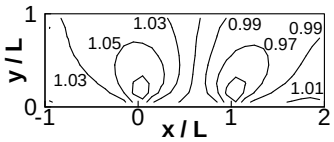

FIGURE 14. n/n_∞ contours for finite plate on small domain ("collisionless" flow, M = 0.4).

The rarefied flows are conventionally categorized into: continuum (Kn < 0.01), slip flow (0.01 < Kn < 0.1), transition (0.1 < Kn < 10) and free molecular regimes (Kn > 10). The simulations presented in this paper cover all these regimes. The highest Reynolds number achieved is 246.27 and the computational time for this case requires maximum usage of computer resources available to this research. The critical Reynolds number to produce turbulence on a flat plate is about 200,000 and, clearly, the present simulations are quite far from that.

The present calculations have been performed using an Intel XEON processor with 2.6 GHz speed and 1 GB memory. A finite plate Kn = 0.02 run requires 25 days and uses 8.1% memory for a sample size of 4×10^5. (Samples are taken every other time step.)

CONCLUSIONS

A subsonic outflow extrapolation scheme is developed for the DSMC simulations by carrying the properties along the streamline trajectories using the Neumann boundary conditions. The outcomes of this study are as follows:

(1) With the present subsonic outflow boundary condition technique, the results show little distortion near the boundaries and the general features of the main flow are correctly calculated. This technique may be used in the simulations for which the characteristic open boundary conditions are not suitable.

(2) The calculations are in very good agreement with the experimental drag coefficient data and theoretical results.

(3) For the present flows, cell sizes in the normal direction (Δy) should be less or equal to the local mean free path for correct results. However, large cell sizes in the streamwise direction (Δx) may be used with reasonable accuracy (*e.g.* if Δx is 5 times the local mean free path, the drag coefficient changes by 3%).

ACKNOWLEDGMENTS

The authors wish to thank Sinan Eyi for his valuable help related with the inflow/outflow boundary conditions.

REFERENCES

1. G. A. Bird, *Molecular Gas Dynamics and Direct Simulation of Gas Flows*, Clarendon Press, Oxford, 1994.
2. R. P. Nance, D. B. Hash and H. A. Hassan, "Role of Boundary Conditions in Monte Carlo Simulation of MEMS Devices", AIAA Paper 97-0375, 1997.
3. M. Ilgaz and M. C. Çelenligil, "DSMC Simulations of Low-Density Choked Flows in Parallel-Plate Channels", RGD:23rd Int. Symp., ed. by A. D. Ketsdever and E. P. Muntz, AIP Conference Proceedings 663, AIP, Melville, NY, 2003, pp. 831-840.
4. Q. Sun and J. D. Boyd, "Drag on a Flat Plate in Low-Reynolds-Number Gas Flows", *AIAA Journal*, **42**, 1066-1072 (2004).
5. V. K. Dogra and J. N. Moss, "Hypersonic Rarefied Flow About Plates at Incidence", *AIAA Journal*, **29**, 1250-1258 (1991).
6. Ö. H. Turgut, "Effects of Extrapolation Boundary Conditions on Subsonic MEMS Flows over a Flat Plate", M.S. Thesis, Middle East Technical University, Ankara, Türkiye, 2006.
7. G. A. Bird, "Monte Carlo Simulation in an Engineering Context", AIAA Progress in Astronautics and Aeronautics: Rarefied Gas Dynamics, edited by Sam S. Fisher, **74**, AIAA, NY, 1981, pp. 239-255.
8. S. A. Schaaf and F. S. Sherman, "Skin Friction in Slip Flow", *Journal of the Aeronautical Sciences*, **21**, 85-90 (1954).